THE ASTROPHYSICAL JOURNAL, 551:L185–L188, 2001 April 20

"SHALLOW-WATER" MAGNETOHYDRODYNAMIC WAVES IN THE SOLAR TACHOCLINE

D. A. SCHECTER,[1] J. F. BOYD, AND P. A. GILMAN
High Altitude Observatory, National Center for Atmospheric Research,[2] P.O. Box 3000, Boulder, CO 80307
Received 2001 January 2; accepted 2001 February 5; published 2001 April 17

ABSTRACT

This Letter discusses waves in a rotating magnetized fluid layer, governed by "shallow-water" magnetohydrodynamics. Such waves likely exist in the solar tachocline, and we focus on this application. A dispersion relation is derived, giving two branches of waves: Alfvén and magnetogravity. In general, finite Alfvén and magnetogravity waves can propagate without change of shape. However, if the Coriolis force is absent, as on the equator of the tachocline, finite magnetogravity waves steepen and develop singularities in a time τ_s. It is shown that τ_s increases monotonically with the ambient magnetic field strength.

Subject headings: MHD — Sun: interior — Sun: magnetic fields — Sun: rotation — waves

1. INTRODUCTION AND BASIC EQUATIONS

Gilman (2000) recently introduced "shallow-water" magnetohydrodynamics (SMHD) as a simple model for understanding predominantly horizontal flows in the solar tachocline. In this complimentary Letter, we examine analytic solutions to SMHD waves in the tachocline. We show that there are two branches of such waves: Alfvén and magnetogravity. Finite Alfvén and magnetogravity waves can both propagate without change of shape in regions of the tachocline where the Coriolis force is finite. At the equator, where the Coriolis force is zero, magnetogravity waves steepen and develop singularities (De Sterck 2001). We show that the time required for a singularity to form increases with the ambient magnetic field strength.

The tachocline (Spiegel & Zahn 1992) is a thin layer of the solar interior, straddling the convection zone and the radiative interior. It is widely believed that a toroidal magnetic field of at least 10^5 G permeates this layer (e.g., Moreno-Insertis, Schüssler, & Ferriz-Mas 1992). The tachocline naturally divides into two sublayers: an inner "radiative" layer and an outer "overshoot" layer. By current estimates, the radiative layer is twice as thick as the overshoot layer. Both sublayers have stable subadiabatic temperature gradients, but that of the overshoot layer is much closer to adiabatic.

Here we are interested in the horizontal propagation of waves in either sublayer. We will use ideal SMHD (Gilman 2000) to describe these waves. In this model, a sublayer is viewed as an inviscid, incompressible, perfectly conducting fluid, with a rigid base and a free upper surface. The magnetic field is tangent to the base and to the upper surface. The subadiabatic stratification in the sublayer provides some negative buoyancy, which is represented by a reduced gravitational force. The total vertical pressure gradient (fluid plus magnetic) is regarded as hydrostatic. This implies that the total horizontal pressure gradient is determined by the inclination of the free upper surface.

We restrict our attention to regions of the tachocline that span less than about 10° latitude and longitude. In such regions, we may view a sublayer as having rectangular (slab) geometry. Therefore, it is reasonable to use a local Cartesian (x, y, z) coordinate system for analysis, as illustrated in Figure 1. Here $\hat{z}$ points vertically upward, against gravity. When discussing horizontal wave propagation, we will set $\hat{x}$ parallel to the wavevector $\boldsymbol{k}$ (Fig. 1*b*). This differs from standard practice, where $\hat{x}$ is parallel to the background magnetic field.

Let $H(x, y, t)$ denote the thickness of the sublayer, and $\boldsymbol{u}(x, y, t)$ denote the horizontal velocity field within the sublayer. In addition, let $\boldsymbol{B}(x, y, t)$ denote the horizontal magnetic field divided by $(4\pi\rho)^{1/2}$, where ρ is the average (approximately constant) mass density of the sublayer. In ideal SMHD, the horizontal momentum, horizontal induction, and mass continuity equations are (in order)

$$\begin{aligned} \partial_t \boldsymbol{u} &= -\boldsymbol{u}\cdot\nabla\boldsymbol{u} + \boldsymbol{B}\cdot\nabla\boldsymbol{B} - g_r\nabla H + f\boldsymbol{u}\times\hat{z}, \\ \partial_t \boldsymbol{B} &= -\boldsymbol{u}\cdot\nabla\boldsymbol{B} + \boldsymbol{B}\cdot\nabla\boldsymbol{u}, \qquad \partial_t H = -\nabla\cdot H\boldsymbol{u}, \end{aligned} \tag{1}$$

where $\nabla \equiv \hat{x}\partial_x + \hat{y}\partial_y$, g_r is the reduced gravity, and f is the Coriolis parameter. We have added a Coriolis term to the momentum equation of Gilman (2000), since our coordinate system is fixed on a rotating Sun. The value of f is 2 times the local vertical rotation frequency of the Sun (e.g., $f = 0$ on the equator). In the limit where $\boldsymbol{B} = 0$, equations (1) reduce to the shallow-water "*f*-plane" equations of geophysical fluid dynamics (Gill 1982). In addition to equations (1), the boundary condition that $\boldsymbol{B}$ is tangent to the free upper surface leads to the following constraint (Gilman 2000):

$$\nabla\cdot H\boldsymbol{B} = 0. \tag{2}$$

The reduced gravity approximation that is used in SMHD is common in layer models of atmospheric and oceanographic flows (e.g., Ripa 1991; Gill 1982). Gilman (2000) argued that the reduced gravity g_r appropriate to a sublayer of the tachocline is of order αg, where g is the local solar gravity and α is the fractional difference between an adiabatic temperature gradient and the actual temperature gradient of the sublayer. For the radiative layer, we estimate that $0.01 \lesssim \alpha \lesssim 0.3$, whereas for the overshoot layer, we estimate that $10^{-6} \lesssim \alpha \lesssim 10^{-4}$. These numbers are based on a "standard model" for the structure of the solar interior, calibrated by helioseismic results by Christensen-Dalsgaard (1998), and were obtained from him through private communication.

Note that one-layer SMHD ignores the fact that the tachocline has vertical shear in velocity, and possibly magnetic field. We further ignore mean horizontal shears. This greatly simplifies our analysis of neutral waves. We expect that neutral

[1] Advanced Study Program postdoctoral fellow working in part at the High Altitude Observatory; daspla@ucar.edu.
[2] The National Center for Atmospheric Research is supported by the National Science Foundation.

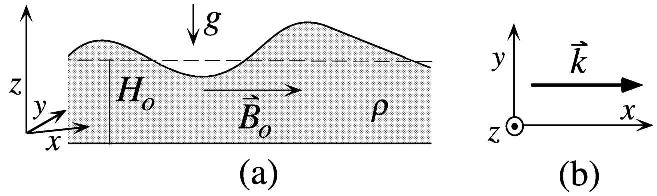

FIG. 1.—(*a*) Sublayer of the solar tachocline with average density ρ, equilibrium thickness H_0, and equilibrium magnetic field $\boldsymbol{B}_0$. (*b*) Orientation of the *x*-, *y*-, and *z*-axes relative to the wavevector $\boldsymbol{k}$.

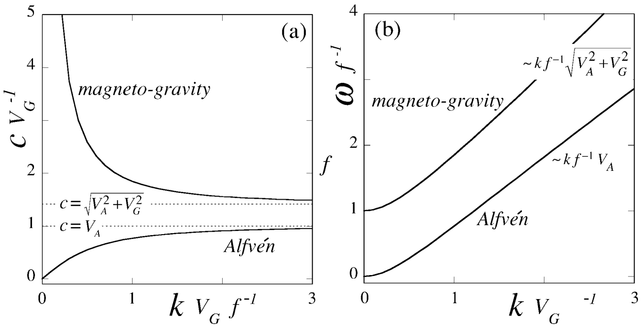

FIG. 2.—Dispersion curves for linear SMHD waves, with $V_A = V_G$. (*a*) Phase speed vs. wavenumber. (*b*) Frequency vs. wavenumber.

waves with the same restoring forces exist when shear is present, but along with unstable modes (Dikpati & Gilman 2001).

2. LINEAR WAVES

Consider a sublayer of the tachocline that initially has a uniform thickness H_0, a uniform horizontal magnetic field $\boldsymbol{B}_0$, and is at rest (in the rotating frame). Let h and $\boldsymbol{b}$ denote the layer thickness and horizontal magnetic field perturbations; that is, $h \equiv H - H_0$ and $\boldsymbol{b} \equiv \boldsymbol{B} - \boldsymbol{B}_0$. For now, we assume that the perturbation fields (including $\boldsymbol{u}$) are small, so that second-order terms in equations (1) and (2) can be ignored. The resulting linearized equations have a complete basis of sinusoidal wave solutions: $\boldsymbol{u}$, $\boldsymbol{b}$, $h \propto e^{i(kx-\omega t)}$. Here k and ω are the constant wavenumber and wave frequency, respectively. We have oriented the x-axis to run parallel to the wavevector $\boldsymbol{k}$ (Fig. 1*b*).

The dispersion relation for the linear waves is the following:

$$\omega_{\pm}^2 = k^2 V_A^2 + \frac{f^2}{2} + \frac{V_G^2}{2}\left[k^2 \pm \sqrt{\frac{f^4}{V_G^4} + k^2\left(2\frac{f^2}{V_G^2} + 4\frac{f^2 V_A^2}{V_G^4}\right) + k^4}\,\right]. \quad (3)$$

Here $V_A \equiv |\hat{x}\cdot\boldsymbol{B}_0|$ is the Alfvén speed associated with the x-component of the unperturbed magnetic field and $V_G \equiv (g_r H_0)^{1/2}$ is the gravity wave speed in an unmagnetized layer. The dependence of ω on the direction of propagation is contained in V_A.

The dispersion relation in equation (3) has a fast (ω_+) and slow (ω_-) branch, as illustrated in Figure 2. We refer to the fast and slow branches as the "magnetogravity" branch and the "Alfvén" branch, respectively. With zero ambient magnetic field ($V_A = 0$), magnetogravity waves reduce to the well-known "Poincaré waves" of geophysical fluid dynamics (Gill 1982). Like Poincaré waves, magnetogravity waves cover phenomena that occur over timescales less than $2\pi/f$. Of course, Alfvén waves require a nonzero magnetic field to exist. Furthermore, unlike magnetogravity waves, Alfvén waves can account for arbitrarily slow dynamics at large spatial scales ($k \to 0$).

For both branches of linear waves, the perturbation fields are related by the following:

$$\hat{x}\cdot\boldsymbol{u} = \frac{c}{H_0}h, \qquad (c^2 - V_A^2)\boldsymbol{u} - \hat{x}V_G^2\hat{x}\cdot\boldsymbol{u} = \frac{fc}{ik}\hat{z}\times\boldsymbol{u},$$

$$\boldsymbol{b} = -\frac{\hat{x}\cdot\boldsymbol{B}_0}{c}\boldsymbol{u}. \quad (4)$$

Here $c \equiv \omega/k$ is the phase velocity of the wave. If f/k is zero, the Alfvén waves all propagate with phase speed $|c| = V_A$. Substituting this phase speed into equation (4) yields $h = \hat{x}\cdot\boldsymbol{u} = \hat{x}\cdot\boldsymbol{b} = 0$. That is, the Alfvén waves are flat and transverse in the absence of rotation. Their restoring mechanism is magnetic tension. In addition, if f/k is zero, the magnetogravity waves all propagate with phase speed $|c| = (V_A^2 + V_G^2)^{1/2}$. Substituting this phase speed into equation (4) yields $\hat{y}\cdot\boldsymbol{u} = \hat{y}\cdot\boldsymbol{b} = 0$; that is, the horizontal velocity and magnetic field perturbations are aligned with the direction of propagation. The restoring mechanism of a magnetogravity wave involves a combination of fluid pressure and magnetic forces.

We now estimate typical oscillation periods implied by equation (3), for both the radiative and overshoot layers of the tachocline. We assume that both layers have mass density ρ of about 0.2 g cm^{-3} and that both contain a 10^5 G horizontal magnetic field. These parameters give an Alfvén speed of $V_A \simeq 6 \times 10^4$ cm s^{-1}, for waves propagating parallel (or antiparallel) to $\boldsymbol{B}_0$. In addition, we consider disturbances at a latitude of 30°, where $f \simeq 2.6 \times 10^{-6}$ s^{-1}.

The nonmagnetic gravity wave speed, $V_G \equiv (g_r H_0)^{1/2}$, changes appreciably between the two layers. To begin with, the radiative layer is twice as thick as the overshoot layer, which has $H_0 \simeq 5 \times 10^8$ cm. Moreover, g_r is 500–1.5 × 10^4 cm s^{-2} in the radiative layer, whereas g_r is 0.05–5 cm s^{-2} in the overshoot layer. This means that V_G is 7 × 10^5–4 × 10^6 cm s^{-1} in the radiative layer, whereas V_G is 5 × 10^3–5 × 10^4 cm s^{-1} in the overshoot layer.

Our Cartesian model is reasonable only for wavenumbers greater than about $k = 2\pi/0.1R_t = 1.3 \times 10^{-9}$ cm^{-1}, where $R_t \simeq 0.7\ R_\odot$ is the mean radius of the tachocline. Larger scale perturbations are affected by the tachocline's curvature. We may substitute this value of k into equation (3), along with our previous estimates of f, V_A, and V_G, to obtain "typical" wave periods ($2\pi/\omega$). In the radiative layer, where $V_G \gg V_A$, the magnetogravity waves have periods on the order of 1 hr, whereas the Alfvén waves have periods on the order of 1 day. In the overshoot layer, where $V_A \gtrsim V_G$, both the magnetogravity and Alfvén waves have periods on the order of 1 day. Of course, Alfvén waves that propagate nearly perpendicular to $\boldsymbol{B}_0$ have $V_A \simeq 0$ and nearly infinite periods.

3. NONLINEAR WAVES

We now generalize the linear periodic wave solutions to finite amplitude. Ball (1960) has carried out a similar analysis of nonlinear shallow-water waves without magnetic fields.

We look for solutions to the fully nonlinear SMHD equations

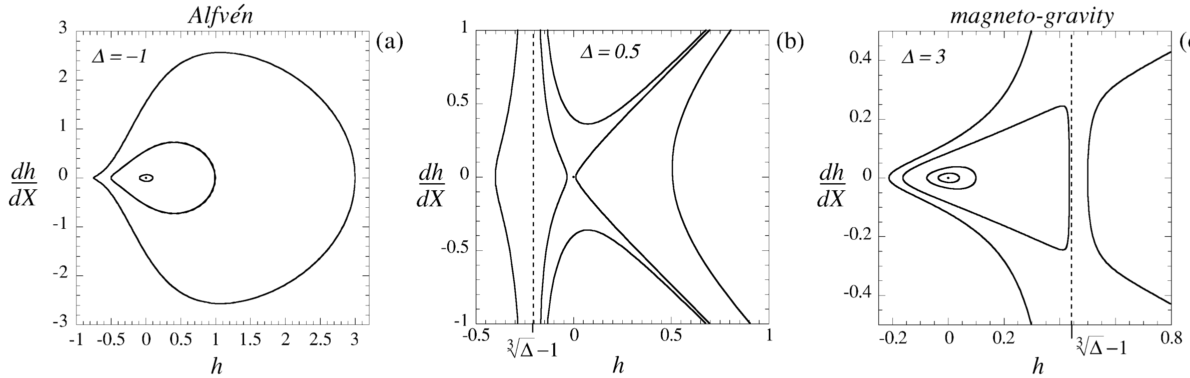

FIG. 3.—Sample phase-space diagrams for each regime of Δ. (*a*) Family of Alfvén waves ($\Delta < 0$). (*b*) If $0 < \Delta < 1$, there are no periodic wave solutions (*closed curves*). (*c*) Family of magnetogravity waves ($\Delta > 1$).

of the form $\boldsymbol{u}(\xi)$, $\boldsymbol{b}(\xi)$, $h(\xi)$, where $\xi \equiv x - ct$. Then, equations (1) and (2) become the following:

$$c\frac{d\boldsymbol{u}}{d\xi} = \hat{x}\cdot\boldsymbol{u}\frac{d\boldsymbol{u}}{d\xi} - \hat{x}\cdot(\boldsymbol{B}_0 + \boldsymbol{b})\frac{d\boldsymbol{b}}{d\xi} + \hat{x}g_r\frac{dh}{d\xi} + f\hat{z}\times\boldsymbol{u}, \qquad (5a)$$

$$c\frac{d\boldsymbol{b}}{d\xi} = \hat{x}\cdot\boldsymbol{u}\frac{d\boldsymbol{b}}{d\xi} - \hat{x}\cdot(\boldsymbol{B}_0 + \boldsymbol{b})\frac{d\boldsymbol{u}}{d\xi}, \qquad (5b)$$

$$ch - (H_0 + h)\hat{x}\cdot\boldsymbol{u} = \text{constant}, \qquad (5c)$$

$$h\hat{x}\cdot\boldsymbol{B}_0 + (H_0 + h)\hat{x}\cdot\boldsymbol{b} = \text{constant}. \qquad (5d)$$

For the linear waves of § 2, the x-components of $\boldsymbol{u}$ and $\boldsymbol{b}$ are zero when h is zero. We impose the same constraints on the nonlinear waves; that is, we require the constants to be zero on the right-hand sides of equations (5c) and (5d). Note that solitons, whose perturbation fields all vanish as $\xi \to \pm\infty$, satisfy these constraints; however, we have found no soliton solutions.

Equations (5a)–(5d) can be rewritten in a form that is more convenient for analysis. To begin with, we introduce the following dimensionless quantities:

$$X \equiv \frac{fc}{V_G^2}(x - ct), \qquad \Delta \equiv \frac{c^2 - V_A^2}{V_G^2}. \qquad (6)$$

Note that the value of Δ is determined by the phase speed of the wave. We also scale the perturbation fields as follows:

$$h \to h/H_0, \qquad \boldsymbol{u} \to \boldsymbol{u}/c, \qquad \boldsymbol{b} \to \boldsymbol{b}/(\hat{x}\cdot\boldsymbol{B}_0). \qquad (7)$$

Then, in a straightforward manner, we convert equations (5a)–(5d) into the following *dimensionless* equations:

$$\frac{d}{dX}\left\{\left[1 - \frac{\Delta}{(1+h)^3}\right]\frac{dh}{dX}\right\} - \frac{h}{\Delta} = 0, \qquad (8a)$$

$$\boldsymbol{u} = \hat{x}\frac{h}{1+h} + \hat{y}\left[1 - \frac{\Delta}{(1+h)^3}\right]\frac{dh}{dX}, \qquad \boldsymbol{b} = -\boldsymbol{u}. \qquad (8b)$$

The wave form is completely determined by equation (8a) for h. Given a solution for h, the velocity and magnetic field perturbations are obtained simply from equations (8b).

We will consider the solutions to equations (8a) and (8b) separately for $\Delta < 0$, $0 < \Delta < 1$, and $\Delta > 1$. If $\Delta < 0$, so that $|c| < V_A$, the solutions include a set of finite periodic waves that stem from the Alfvén branch of linear waves. If $\Delta > 1$, so that $|c| > (V_A^2 + V_G^2)^{1/2}$, the solutions include a set of finite periodic waves that stem from the magnetogravity branch. If $0 < \Delta < 1$, there are no periodic wave solutions, as in linear theory.

A periodic wave can be represented as a closed curve in (h, dh/dX) phase space. Multiplying equation (8a) by $\hat{y}\cdot\boldsymbol{u}$ (eq. [8b]), and integrating, we obtain the following equation for a phase-space curve:

$$\left(\frac{dh}{dX}\right)^2\left[1 - \frac{\Delta}{(1+h)^3}\right]^2 - \frac{h^2}{\Delta} - \frac{1+2h}{(1+h)^2} = \epsilon, \qquad (9)$$

where ϵ is a constant related to the amplitude of the wave. Figure 3 shows phase-space curves for each of the three classes of Δ. Figure 3*b* illustrates that there are no periodic waves (*closed curves*) if $0 < \Delta < 1$.

Figure 3*a* shows a family of nonlinear Alfvén waves ($\Delta < 0$). The small ellipse near the origin corresponds to a sinusoidal wave, consistent with linear theory. For larger amplitude periodic waves (*closed curves*), the height of the peak is generally greater than the depth of the trough. This asymmetry increases with the peak height. However, from equation (8a), the structure of a periodic wave is constrained by

$$\oint dXh = \oint dX\frac{d}{dX}\left\{\left[\Delta - \frac{\Delta^2}{(1+h)^3}\right]\frac{dh}{dX}\right\} = 0, \qquad (10)$$

where $\oint$ denotes integration over a wavelength. That is, the area under the wave is zero. Figure 4*a* illustrates how an Alfvén wave varies with X and amplitude. These plots were obtained from numerical integrations of equation (8a).

Figure 3*c* shows a family of nonlinear magnetogravity waves ($\Delta > 1$). As before, the small ellipse near the origin corresponds to a sinusoidal wave, consistent with linear theory. However, unlike the Alfvén waves, the periodic magnetogravity waves (*closed curves*) are restricted to a maximum height perturbation of $h_* = \Delta^{1/3} - 1$. This value of h_* corresponds to a singular point of equation (8a). Figure 4*b* illustrates how a magneto-

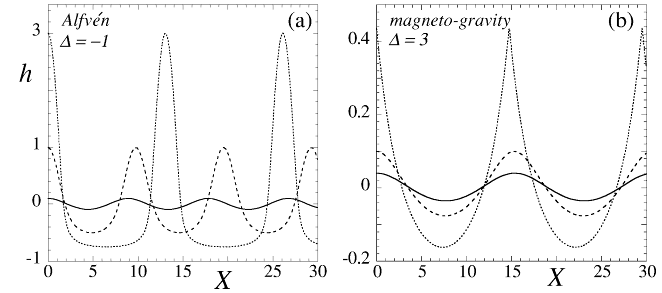

FIG. 4.—(*a*) Nonlinear Alfvén waves and (*b*) nonlinear magnetogravity waves. At small amplitudes, the waves are approximately sinusoidal (*solid curves*), consistent with linear theory. h is normalized to H_0.

gravity wave varies with X and amplitude. Note that the peak develops a cusp as its amplitude increases toward h_*. This singular limit appears to be unphysical, since it suggests an infinite Maxwell stress. We believe that the cusp is an artifact of neglecting small length scales in the "shallow-water" approximation (Gilman 2000).

We have yet to examine the stability of the nonlinear SMHD waves described here. A related issue, which may be resolved in future work, is the extent to which arbitrary initial conditions evolve to these waves.

4. STEEPENING AT THE EQUATOR

In § 3, we showed that linear SMHD waves have finite amplitude generalizations that propagate without change of shape. We will refer to such waves as "permanent." However, our analysis assumed nonzero f. We find that, at the equator of the tachocline, where $f = 0$, the permanent nonlinear wave equations (eqs. [5a]–[5d]) have no regular solutions, unless $h = 0$. This suggests that a finite magnetogravity wave, whose restoring mechanism requires nonzero h, will steepen and develop singularities. This steepening has already been pointed out by De Sterck (2001), who examined the hyperbolic theory of SMHD for a nonrotating magnetofluid. Here we add a calculation of the time required for a singularity to develop.

To begin with, we consider a more general class of nonlinear waves: the so-called "simple waves" (Lighthill 1978). By definition, all components of a simple wave ($\boldsymbol{u}$, $\boldsymbol{b}$, h) are determined by a single component. For example, the velocity and magnetic field perturbations of a simple magnetogravity wave are both functions of $h(x, t)$. In order to be consistent with linear theory, we also require that, on the equator, the horizontal components of a simple magnetogravity wave be aligned with the direction of propagation; that is, $\hat{y}\cdot\boldsymbol{u} = \hat{y}\cdot\boldsymbol{b} = 0$.

One can easily check, using equations (1) with $f = 0$, that such simple magnetogravity waves satisfy the following *dimensional* equations:

$$\partial_t h + U_\pm(h)\partial_x h = 0,$$
$$\boldsymbol{u}_\pm = \pm\hat{x}V_G\int_1^{1+h/H_0} d\chi\sqrt{\frac{1}{\chi} + \frac{V_{\rm A}^2}{V_G^2}\frac{1}{\chi^4}},$$
$$\boldsymbol{b} = -\hat{x}(\hat{x}\cdot\boldsymbol{B}_0)\frac{h}{H_0 + h}. \qquad (11)$$

Here χ is a dummy variable and

$$U_\pm(h) \equiv \frac{d}{dh}[(H_0 + h)\hat{x}\cdot\boldsymbol{u}_\pm]. \qquad (12)$$

The characteristic speed $U_\pm(h)$ is a monotonically increasing (U_+) or decreasing (U_-) function of h. Consequently, an infinite slope will form on the leading edge of the wave in a finite time τ_s.

The value of τ_s is given by min $|\partial_x h\, dU/dh|^{-1}$; i.e.,

$$\tau_s = \min\left|\frac{2H_0}{3V_G}\frac{\sqrt{(V_{\rm A}^2/V_G^2) + (1 + h/H_0)^3}}{(1 + h/H_0)\partial_x h}\right|. \qquad (13)$$

Here "min" denotes the minimum along the leading edge of the initial waveform. The singularity formation time τ_s diverges as the magnetogravity wave broadens, i.e., as $\partial_x h$ approaches zero. Furthermore, τ_s increases with $V_{\rm A}$, the magnetic field strength in the direction of propagation. For $V_{\rm A} = 0$, the right-hand side of equation (13) reduces to the established nonmagnetic result, min $|2(H_0 H)^{1/2}/3V_G\partial_x h|$ (e.g., Lighthill 1978, pp. 148–151).

Unlike magnetogravity waves, finite Alfvén waves do not steepen on the equator of the tachocline, where $f = 0$. De Sterck (2001) has shown that, in the absence of rotation, there is an infinite set of permanent nonlinear Alfvén waves with $|c| = V_{\rm A}$. As in the $f = 0$ limit of linear theory, these Alfvén waves are flat and transverse; that is, $h = \boldsymbol{u}\cdot\hat{x} = \boldsymbol{b}\cdot\hat{x} = 0$. In addition, $\boldsymbol{u} = \pm\boldsymbol{b}$, where $+/-$ is for waves propagating antiparallel/parallel to the x-component of $\boldsymbol{B}_0$. This result is easily verified by setting c equal to $\pm V_{\rm A}$ in equations (5a)–(5d) and performing some minor algebra.

In summary, we examined linear and nonlinear SMHD waves in the tachocline. North and south of the equator, where $|f| > 0$, both Alfvén and magnetogravity waves can propagate without change of shape. In contrast, magnetogravity waves steepen at the equator. In this sense, we see that the Coriolis force inhibits steepening. Future work may examine SMHD waves in models in which the tachocline has horizontal velocity shear, horizontal magnetic shear, and curvature.

We thank K. MacGregor for his helpful comments. P. A. Gilman was supported in part by NASA award W-19752. J. F. Boyd was supported at HAO as an undergraduate intern.

REFERENCES

Ball, F. K. 1960, J. Fluid Mech., 9, 506
Christensen-Dalsgaard, J. 1998, Space Sci. Rev., 85, 19
De Sterck, H. 2001, Phys. Plasmas, submitted
Dikpati, M., & Gilman, P. A. 2001, ApJ, in press
Gill, A. E. 1982, Atmosphere-Ocean Dynamics (New York: Academic)
Gilman, P. A. 2000, ApJ, 544, L79
Lighthill, J. 1978, Waves in Fluids (Cambridge: Cambridge Univ. Press)
Moreno-Insertis, F., Schüssler, M., & Ferriz-Mas, A. 1992, A&A, 264, 686
Ripa, P. 1991, J. Fluid Mech., 222, 119
Spiegel, E. A., & Zahn, J.-P. 1992, A&A, 265, 106